A UV non-hydrogen pure selenite nonlinear optical material for achieving balanced properties through framework-optimized structural transformation

Peng-Fei Li[a,b], Chun-Li Hu[a], Jiang-Gao Mao[a,b], Fang Kong[*,a,b]

[a] State Key Laboratory of Structural Chemistry, Fujian Institute of Research on the Structure of Matter, Chinese Academy of Sciences, Fuzhou 350002, P. R. China.
[b] University of Chinese Academy of Sciences, Beijing 100049, P. R. China.

[*]Corresponding Authors: kongfang@fjirsm.ac.cn

Supporting Information

S1. Experimental Section

Materials and Instrumentations.

All the chemicals were obtained from commercial sources and used without further purification: SeO_2 (Adamas-beta, 99.999%), Na_2CO_3 (Adamas-beta, 99.99%), $Lu(NO_3)_3 \cdot 6H_2O$ (Adamas-beta, 99.99%),.

Powder X-ray diffraction (PXRD) patterns of $NaLu(SeO_3)_2$ was collected on the Miniflex 600 powder X-ray diffractometer using Cu Kα radiation (λ = 1.54186 Å) at room temperature in the angular range of 2θ = 5-70° with a scan step size of 0.02°.

Microprobe elemental analysis was carried out with the aid of a field-emission scanning electron microscope (JSM6700F) outfitted with an energy-dispersive X-ray spectroscope (Oxford INCA).

IR spectra was carried out on a Magna 750 FT-IR spectrometer using air as background in the range of 4000–400 cm^{-1} with a resolution of 2 cm^{-1} at room temperature.

The UV-vis-NIR spectra was obtained at 2000–200 nm by a PerkinElmer Lambda 900 spectrophotometer using $BaSO_4$ as the reference, and the reflection spectra were converted into an absorption spectrum using the Kubelka-Munk function. Absorption data was calculated from the diffuse reflection data by the Kubelka-Munk function: $\alpha/S = (1-R)^2/2R$, where α and S represent the absorption coefficient and the scattering coefficient, respectively. The band gap value can be given by extrapolating the absorption edge to the baseline in the α/S vs. energy graph[1].

Thermogravimetric analyses (TGA) were measured by Netzsch STA 499C installation. The

samples about 2.0-5.0 mg were placed in alumina crucibles and heated in 20-1200 °C at a rate of 15 °C/min under N_2 atmosphere.

Powder SHG measurements were conducted using a modified method of Kurtz and Perry[2]. Irradiation laser (λ = 1064 nm) is generated by a Nd:YAG solid-state laser equipped with a Q switch. The $NaLu(SeO_3)_2$ pure crystal samples ground into powder were sieved according to seven different particle size ranges (25−45, 45−53, 53−75, 75−105, 105−150, 150−210 and 210−300 μm). KH_2PO_4 (KDP) samples in the same size range were also be prepared, which were used as reference. SHG signals oscilloscope traces of $NaLu(SeO_3)_2$ and KDP samples in the particle size range (150−210 μm) were recorded.

The LIDT measurements of the $NaLu(SeO_3)_2$ crystal samples and KH_2PO_4 (KDP) samples were performed by a Q-switched pulsed laser. The particle size range of the tested sample was 150−210 μm, the laser wavelength was 1064 nm, the pulse duration was 10 ns, the pulse frequency was 1 Hz, and the laser spot area focused on the sample was 1.54 mm^2. The energy of the laser emission was gradually increased during the measurement, and the LIDT of the sample was determined when it turned black under the laser.

Syntheses

$NaLu(SeO_3)_2$ was synthesized by mild temperature hydrothermal method. A mixture of $Lu(NO_3)_3·6H_2O$ (469.1 mg, 1 mmol), SeO_2 (444.4 mg, 4 mmol), Na_2CO_3(424.0 mg, 1 mmol) and H_2O (5 ml) was sealed in an autoclave containing Teflon liner equipped (23 ml), heated at 225 °C for 5760 minutes, and then slowly cooled to room temperature in 4320 minutes. The products were separated by vacuum filtration, washed with alcohol and dried in air at room

temperature. The transparent needle-like $NaLu(SeO_3)_2$ crystal was obtained in a single pure phase, with a yield of about 87% (based on Se), its purity was confirmed by X-ray diffraction (XRD) studies (Figure S1).

S2. Single-crystal X-ray diffraction

Single crystal X-ray diffraction data were obtained on Agilent Technologies SuperNova dual-wavelength CCD diffractometer with a graphite-monochromated Mo Kα radiation (λ = 0.71073 Å) at room temperature. Data reduction and cell refinement and were performed with *CrysAlisPro*. The structure was solved by the direct methods and refined by full-matrix least-squares fitting on F^2 using *OLEX2-1.5* crystallographic software package[3, 4]. All atoms were refined with anisotropic thermal parameters. The structural data were also checked by PLATON and no higher symmetry was found[5]. The detailed crystallographic data was given in Table S1. The bond lengths were listed in Table S2[6, 7].

S3. Computational Method

Single-crystal structural data of $NaLu(SeO_3)_2$ was used for the theoretical calculations. The electronic structures were performed using a plane-wave basis set and pseudo-potentials within density functional theory (DFT) implemented in the total-energy code CASTEP[8]. For the exchange and correlation functional, we chose Perdew–Burke–Ernzerhof (PBE) in the generalized gradient approximation (GGA). The interactions between the ionic cores and the electrons were described by the ultrasoft pseudopotential. The following valence-electron configurations were considered in the computation: Lu-$4f^{14}5d^16s^2$, Se-$4s^24p^4$, O-$2s^22p^4$, and

Na-$2s^2 2p^6 3s^1$. The numbers of plane waves included in the basis sets were determined by cutoff energy of 900 eV. The numerical integration of the Brillouin zone was performed using Monkhorst-Pack k-point sampling of 2 × 3 × 5. The other parameters and convergent criteria were the default values of CASTEP code.

The calculations of linear optical properties in terms of the complex dielectric function $\varepsilon(\omega) = \varepsilon_1(\omega) + i\varepsilon_2(\omega)$ were made. The imaginary part of the dielectric function ε2 was given in the following equation:

$$\varepsilon^{ij}_2(\omega) = \frac{8\pi^2 h^2 e^2}{(m^2 V)} \sum_k \sum_{cv} (f_c - f_v) \frac{p^i_{cv}(k) p^j_{cv}(k)}{E^2_{vc}} \delta [E_c(\mathrm{k}) - E_v(\mathrm{k})\text{-h}\omega]$$

The f_c and f_v represent the Fermi distribution functions of the conduction and valence band. The term $p^i_{cv}(k)$ denotes the momentum matrix element transition from the energy level c of the conduction band to the level v of the valence band at the *k*th point in the Brillouin zone (BZ), and *V* is the volume of the unit cell.

The real part $\varepsilon_1(\omega)$ of the dielectric function $\varepsilon(\omega)$ follows from the Kramer–Kronig relationship. All the other optical constants may be derived from $\varepsilon_1(\omega)$ and $\varepsilon_2(\omega)$. For example, the refractive index $n(\omega)$ can be calculated using the following expression[9]:

$$n(\omega) = \left(\frac{1}{\sqrt{2}}\right)\left[\sqrt{\varepsilon_1^2(\omega) + \varepsilon_2^2(\omega)} + \varepsilon_1(\omega)\right]^{1/2}$$

Table S1. Summary of crystal data and structural refinements for $NaLu(SeO_3)_2$ and $NaGa(SeO_3)_2$.

molecular formula	$NaLu(SeO_3)_2$	$NaGa(SeO_3)_2$[10]
Formula Weight	451.88	346.63
crystal system	orthorhombic	orthorhombic
space group	$Pna2_1$	*Pnma*
Temperature(K)	282.15	173.0(2)
F(000)	792.0	N/A
a/Å	12.7180(5)	12.4545(2)
b/Å	8.3994(3)	5.29670(10)
c/Å	5.3750(2)	7.80440(10)
α(deg)	90	90
β(deg)	90	90
γ(deg)	90	90
V/Å^3	574.18(4)	514.839(14)
Z	4	4
Dc(g.cm^{-3})	5.227	4.472
Flack	0.14(2)	N/A
GOF on F^2	1.000	N/A
R_1,wR_2[I > 2σ(I)]$^\alpha$	R_1 = 0.0200, wR_2 = 0.0416	R_1 = 0.0292
R_1, wR_2 (all data)$^\alpha$	R_1 = 0.0214, wR_2 = 0.0419	R_1 = 0.0636
^{a} $R_1 = \sum\|\|F_o\| - \|F_c\|\|/\sum\|F_o\|$, $wR_2 = \{\sum w[(F_o)^2 - (F_c)^2]^2/\sum w[(F_o)^2]^2\}^{1/2}$		

Table S2. Calculated bond valences for $NaLu(SeO_3)_2$.

Compound	Bond	Bond lengths	Bond-valence	BVS
$NaLu(SeO_3)_2$	Se1-O1	1.692(6)	1.379	4.132
	Se1-O2	1.684(5)	1.410	
	Se1-O3	1.702(6)	1.343	
	Se2-O4	1.672(7)	1.456	4.138
	Se2-O5	1.723(6)	1.269	
	Se2-O6	1.683(6)	1.413	
	Na1-O1#1	2.898(7)	0.051	0.896
	Na1-O2#1	2.515(7)	0.145	
	Na1-O3#2	2.542(7)	0.135	
	Na1-O4	2.514(8)	0.145	
	Na1-O4#3	2.961(9)	0.043	
	Na1-O6#4	2.383(8)	0.207	
	Na1-O6#3	2.455(8)	0.170	
	Lu1-O1#5	2.260(6)	0.458	2.986
	Lu1-O2#6	2.236(5)	0.489	
	Lu1-O3	2.217(6)	0.514	
	Lu1-O4	2.220(7)	0.510	
	Lu1-O5#4	2.559(5)	0.204	
	Lu1-O5#7	2.300(6)	0.411	
	Lu1-O6#4	2.310(6)	0.400	

Symmetry transformations used to generate equivalent atoms:
For $NaLu(SeO_3)_2$: #1 -1/2+X,3/2-Y,-1+Z;#2 -1/2+X,3/2-Y,+Z; #3 1-X,2-Y,1/2+Z; #4 +X,+Y,1+Z; #5 +X,+Y,-1+Z; #6 3/2-X,1/2+Y,-1/2+Z; #7 1-X,1-Y,1/2+Z

Table S3. The reported non-hydrogen selenite compounds with thermal stability ≥ 400℃.

Compounds	Thermal stability	Ref.	Compounds	Thermal stability	Ref.
$HgCu(SeO_3)_2$	400 ℃	11	$Cd_6(PO_4)_{1.34}(SeO_3)_{4.66}$	485 ℃	12
$Ag_5Bi(SeO_3)_4$	400 ℃	13	$LiBa_3Bi_6(SeO_3)_7F_{11}$	485 ℃	14
$A_2Bi_2(SeO_3)_3F_2$ (A=K, Rb)	400 ℃	15	$YVSe_2O_8$	500 ℃	16
$Pb_2GaF_2(SeO_3)_2Cl$	400 ℃	17	$Bi_2F_2(MoO_4)(SeO_3)$	510 ℃	18
$PbMo_2O_5(SeO_3)_2$	400 ℃	19	$Pb_2Cd(SeO_3)_2Br_2$	510 ℃	20
$Cs(TiOF)_3(SeO_3)_2$	402 ℃	21	$Pb_2Cd(SeO_3)_2Cl_2$	516 ℃	20
$Sr(VO_2F)(SeO_3)$	405 ℃	22	$Pb_3(SeO_3)_2Br_2$	530 ℃	23
$Na_2Nb_4O_7(SeO_3)_4$	417 ℃	24	$Lu_3F(SeO_3)_4$	550 ℃	25
$BiGa(SeO_3)_3$	420 ℃	26	$Ba_2Zn(SeO_3)_2Cl_2$	550 ℃	27
$Pb_2GaF_2(SeO_3)_2Br$	425 ℃	28	$BaZn_2(SeO_3)_2Cl_2$	550 ℃	27
$Na_3Ti_3O_3(SeO_3)_4F$	430 ℃	29	$CsY(SeO_3)_2$	570 ℃	30
$Ag_3Ti_3O_3(SeO_3)_4F$	430 ℃	29, 31	**$NaLu(SeO_3)_2$**	**~575 ℃**	*
$LiGa(SeO_3)_2$	430 ℃	10	$Cd_2(SeO_3)F_2$	580 ℃	32
$NaGa(SeO_3)_2$	430 ℃	10	$FeNd_2(SeO_3)_4Cl$	600 ℃	33
$KGa(SeO_3)_2$	430 ℃	10	$Li_6Co(SeO_3)_4$	600 ℃	34
$CsGa(SeO_3)_2$	430 ℃	10	$Li_6Ni(SeO_3)_4$	600 ℃	34
$Pb_2NbO_2(SeO_3)_2Br$	431 ℃	28	$Li_2Zn(SeO_3)_2$	600 ℃	34
$Hg_3(SeO_3)_2(SeO_4)$	439 ℃	35	$NaSc(SeO_3)_2$	600 ℃	36
$Sr_4(VO_2)_2(SeO_3)_4(Se_2O_5)$	440 ℃	37	$CsSc(SeO_3)_2$	600 ℃	36
$BiFe(SeO_3)_3$	445 ℃	38	$RbSc(SeO_3)_2$	620 ℃	36
$Zn_2(SeO_3)F_2$	450 ℃	32	$AY(SeO_3)_2$ (A=K、Rb)	620 ℃	30
$Na_6(W_6O_{19})(SeO_3)_2$	450 ℃	39	$CaYF(SeO_3)_2$	625 ℃	40
$Bi_2(SeO_3)_2(SeO_4)$	450 ℃	41	$KSc(SeO_3)_2$	640 ℃	36
$CdCu(SeO_3)_2$	459 ℃	11	$KNb_3Se_2O_{12}$	690 ℃	24
$CdPb_8(SeO_3)_4Cl_4Br_6$	470 ℃	42	$Y_3F(SeO_3)_4$	690 ℃	40
$Ba_3Bi_{6.5}(SeO_3)_7F_{10.5}O_{0.5}$	477 ℃	14	$Li_6Cd(SeO_3)_4$	~700 ℃	34
$Cd_3(SeO_3)_2(SeO_4)$	482 ℃	35	$Cs(TaO_2)_3(SeO_3)_2$	~700 ℃	21
***This work.**					

Table S4. The reported non-hydrogen pure selenite NLO crystals with *Eg*＞4.2 eV.

Compounds	Space group	SHG efficiency	*Eg* (eV)	Thermal stability	Ref.
$RbScSe_2O_6$	$P6_3mc$	1 × ADP	4.9	620 ℃	36
$NaY(SeO_3)_2$	$Pna2_1$	1 × ADP	4.6	325 ℃	30
$RbSb_3Se_2O_{12}$	$P6_3mc$	1 × KDP	4.27	325 ℃	43
$KSb_3Se_2O_{12}$	$P6_3mc$	1.3 × KDP	4.46	325 ℃	43
$CsSb_3Se_2O_{12}$	$P6_3mc$	1.6 × KDP	4.21	570 ℃	43
$NaLu(SeO_3)_2$	***$Pna2_1$***	**2.7 × KDP**	**5.3**	**~575 ℃**	*
***This work.**					

Table S5. State energies (eV) of the lowest conduction band (L-CB) and the highest valence band (H-VB) of $NaLu(SeO_3)_2$.

Compound	k-point	L-CB	H-VB
$NaLu(SeO_3)_2$	G (0.000, 0.000, 0.000)	4.315597	-0.10334
	Z (0.000, 0.000, 0.500)	4.581841	-0.10172
	T (-0.500, 0.000, 0.500)	4.563254	-0.16705
	Y (-0.500, 0.000, 0.000)	4.311262	-0.12579
	S (-0.500, 0.500, 0.000)	4.386441	-0.18561
	X (0.000, 0.500, 0.000)	4.335269	-0.21557
	U (0.000, 0.500, 0.500)	4.370892	-0.01151
	R (-0.500, 0.500, 0.500)	4.324554	0

Table S6. Calculation of the dipole moments of the SeO_3 and the net dipole moment of a unit cell of $NaGa(SeO_3)_2$ and $NaLu(SeO_3)_2$. (D = Debyes).

$NaGa(SeO_3)_2$				
Polar unit	Dipole moment (D)			
	total magnitude	x-component	y-component	z-component
$Se(1)O_3$	9.355	9.304	0	0.971
	9.355	9.304	0	-0.971
	9.355	-9.304	0	0.971
	9.355	-9.304	0	-0.971
Net dipole moment of $Se(1)O_3$	0	0	0	0
$0.5 \times Se(2)O_3$	10.387	7.484	0	7.203
	10.390	-7.487	0	-7.205
	10.390	7.487	0	7.205
	10.387	-7.484	0	-7.203
$Se(2)O_3$	10.385	7.482	0	-7.203
	10.385	-7.482	0	7.203
Net dipole moment of $Se(2)O_3$	0	0	0	0
Net dipole moment (a unit cell)	0	0	0	0
$NaLu(SeO_3)_2$				
Polar unit	Dipole moment (D)			
	total magnitude	x-component	y-component	z-component
$Se(1)O_3$	9.015	6.726	5.924	-0.964
	9.016	-6.727	5.924	-0.963
	9.011	-6.723	-5.922	-0.964
	9.016	6.727	-5.924	-0.963
Net dipole moment of $Se(1)O_3$	3.854	0.003	0.002	-3.854
$Se(2)O_3$	9.812	-9.809	-0.021	-0.243
	9.812	9.809	0.021	-0.242
	9.812	-9.809	0.021	-0.243
	9.812	9.809	-0.021	-0.242
Net dipole moment of $Se(2)O_3$	0.969	0	0	-0.969
Net dipole moment (a unit cell)	4.823	0.003	0.002	-4.823

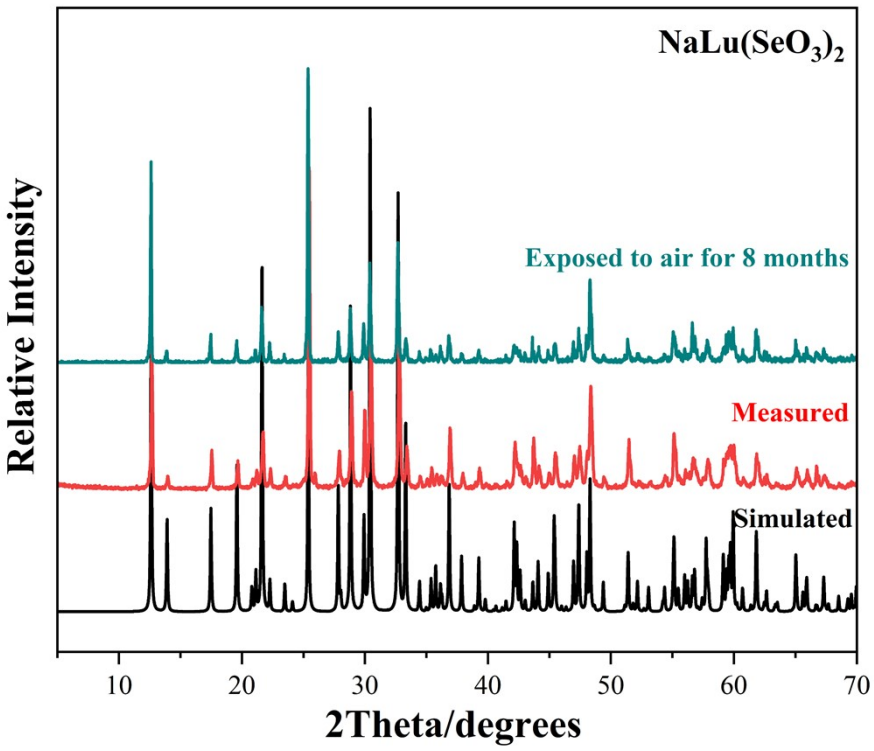

Figure S1. Simulated and experimental powder X-ray diffractometer patterns of $NaLu(SeO_3)_2$.

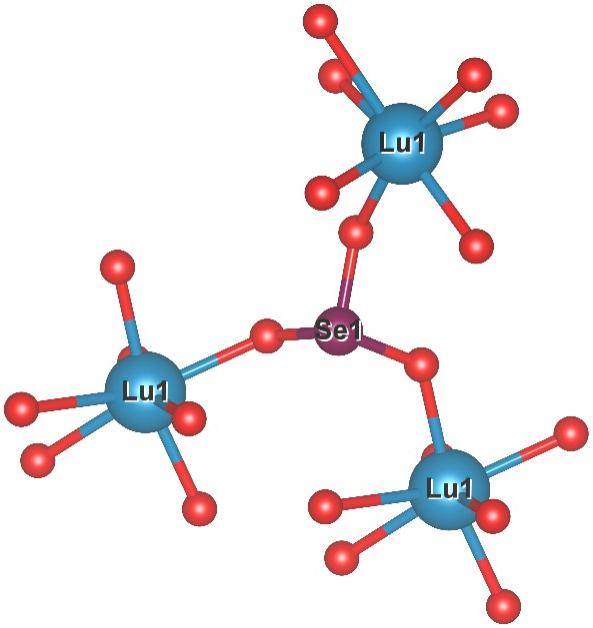

(a)

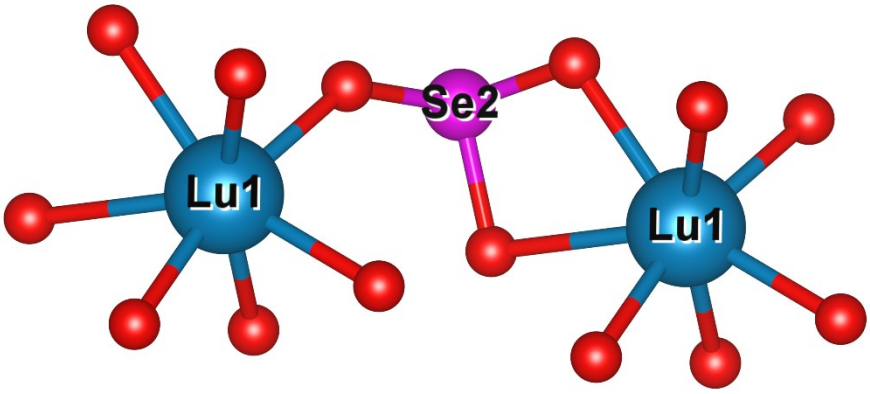

(b)

Figure S2. The coordination environments of $Se(1)O_3$ group (a) and $Se(2)O_3$ (b) in $NaLu(SeO_3)_2$.

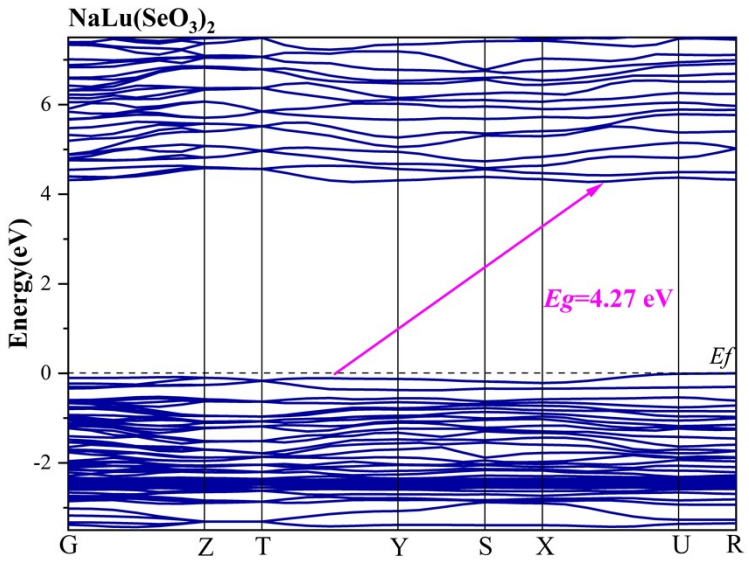

Figure S3. The band structure of $NaLu(SeO_3)_2$.

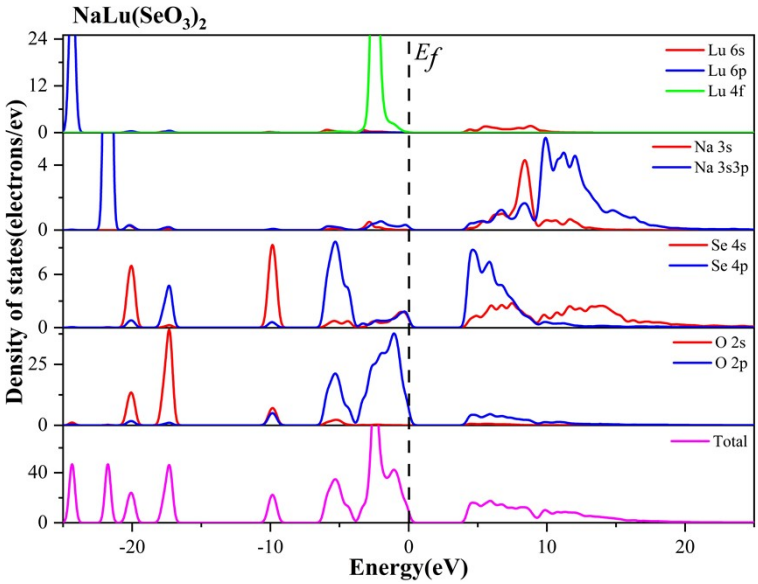

Figure S4. The total and partial density of states for $NaLu(SeO_3)_2$.

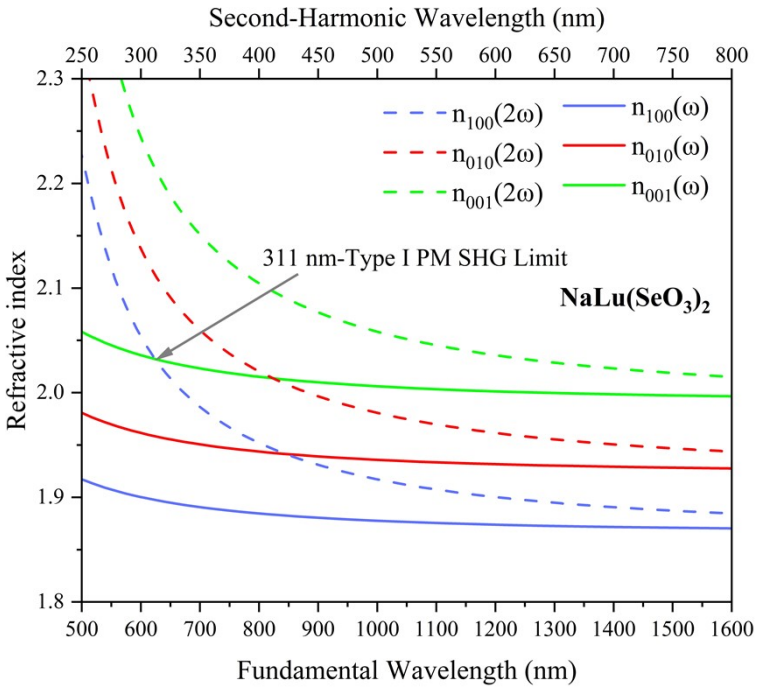

Figure S5. Calculated refractive index dispersion curves and the predicted shortest type I phase-matching (PM) SHG wavelength of $NaLu(SeO_3)_2$.

References

1. P. Kubelka and F. Munk, *Technol. Physical* 1931, **12**, 259−274.
2. S. K. Kurtz and T. T. Perry, *J. Appl. Phys.*, 1968, **39**, 3798-3813.
3. O. V. Dolomanov, L. J. Bourhis, R. J. Gildea, J. A. K. Howard and H. Puschmann, *J. Appl. Cryst.*, 2009, **42**, 339-341.
4. G. M. Sheldrick, *Acta Cryst.*, 2015, **C71**, 3-8.
5. A. L. Spek, *J. Appl. Cryst.*, 2003, **36**, 7−13.
6. B. I. D. BROWN and D. ALTERMATr, *Acta Cryst.*, 1985, **B41**, 244-247.
7. B. N. E. BRESE and M. O'KEEFFE, *Acta Cryst.*, 1991, **B47**, 192-197.
8. S. J. Clark, M. D. Segall, C. J. Pickard, P. J. Hasnip, M. I. J. Probert, K. Refson and M. C. Payne, *Z Kristallogr*, 2005, **220**, 567-570.
9. D. Vanderbilt, *Phys. Rev. B*, 1990, **41**, 7892-7895.
10. D. W. Lee and K. M. Ok, *Inorg. Chem.*, 2013, **52**, 5176-5184.
11. X. L. Cao, F. Kong, Z. Z. He and J. G. Mao, *Dalton Trans.*, 2015, **44**, 11420-11428.
12. Y. X. Ma, Y. P. Gong, C. L. Hu, J. G. Mao and F. Kong, *Inorg. Chem.*, 2018, **262**, 320-326.
13. X. X. Wang, X. B. Li, C. L. Hu, F. Kong and J. G. Mao, *Sci. China. Mater.*, 2019, **62**, 1821-1830.
14. S. S. Shi, C. S. Lin, D. Zhao, M. Luo, L. L. Cao, G. Peng and N. Ye, *Chem. Commun.*, 2021, **57**, 2982-2985.
15. S. S. Shi, C. S. Lin, G. S. Yang, L. L. Cao, B. X. Li, T. Yan, M. Luo and N. Ye, *Chem. Mater.*, 2020, **32**, 7958-7964.
16. Y. H. Kim, D. W. Lee and K. M. Ok, *Inorg. Chem.*, 2014, **53**, 1250-1256.
17. F. G. You, F. Liang, Q. Huang, Z. G. Hu, Y. C. Wu and Z. S. Lin, *J. Am. Chem. Soc.*, 2019, **141**, 748-752.
18. Y. P. Gong, C. L. Hu, F. Kong and J. G. Mao, *Chem. Eur.J.*, 2019, **25**, 3685-3694.
19. S. J. Oh, D. W. Lee and K. M. Ok, *Inorg. Chem.*, 2012, **51**, 5393-5399.
20. Y. P. Gong, C. L. Hu, Y. X. Ma, J. G. Mao and F. Kong, *Inorg. Chem. Front.*, 2019, **6**, 3133-3139.
21. X. L. Cao, C. L. Hu, F. Kong and J. G. Mao, *Inorg. Chem.*, 2015, **54**, 3875-3882.

22. M. L. Liang, Y. X. Ma, C. L. Hu, F. Kong and J. G. Mao, *Dalton Trans.*, 2018, **47**, 1513-1519.

23. X. X. Wang, X. X. Jiang, H. M. Liu, L. Yang, Z. S. Lin, Z. G. Hu, X. G. Meng, X. G. Chen and J. G. Qin, *Dalton Trans.*, 2018, **47**, 1911-1917.

24. X. L. Cao, C. L. Hu, F. Kong and J. G. Mao, *Inorg. Chem.*, 2015, **54**, 10978-10984.

25. C. Wu, L. H. Li, L. Lin, Z. P. Huang, M. G. Humphrey and C. Zhang, *Chem. Mater.*, 2020, **32**, 3043-3053.

26. Y. X. Ma, Y. P. Gong, C. L. Hu, F. Kong and J. G. Mao, *Inorg. Chem.*, 2020, **59**, 7852-7859.

27. Q. Li, L. Geng, H.-Y. Lu, K. Dai and W.-D. Cheng, *J. Solid State Chem.*, 2018, **265**, 117-122.

28. H. Zhao, P. Gong, X. Zhang, Z. Lin, Z. Hu and Y. Wu, *Dalton Trans.*, 2020, **49**, 14046-14051.

29. S. N. Yan, X. X. Wang, C. L. Hu, B. X. Li, F. Kong and J. G. Mao, *Inorg. Chem.*, 2022, **61**, 2686-2694.

30. S. E. Bang, D. W. Lee and K. M. Ok, *Inorg. Chem.*, 2014, **53**, 4756-4762.

31. Q. Qian, F. Kong and J. G. Mao, *RSC Adv.*, 2016, **6**, 79681-79687.

32. F. You, P. Gong, F. Liang, X. Jiang, H. Tu, Y. Zhao, Z. Hu and Z. Lin, *CrystEngComm*, 2019, **21**, 2485-2489.

33. Y. Xie, Z. He, W. Zhang, Z. Zhao, M. Zhang and X. Huang, *J. Solid State Chem.*, 2020, **286**.

34. H. Jo, S. Lee, K. Y. Choi and K. M. Ok, *Inorg. Chem.*, 2018, **57**, 3465-3473.

35. M. Shang and P. S. Halasyamani, *J. Solid State Chem.*, 2020, **286**, 121292.

36. S. Y. Song and K. M. Ok, *Inorg. Chem.*, 2015, **54**, 5032-5038.

37. J. Yeon, S. H. Kim, S. D. Nguyen, H. Lee and P. S. Halasyamani, *Inorg. Chem.*, 2012, **51**, 609-619.

38. S. Y. Zhang, C. L. Hu, P. X. Li, H. L. Jiang and J. G. Mao, *Dalton Trans.*, 2012, **41**, 9532-9542.

39. S. D. Nguyen and P. S. Halasyamani, *Inorg. Chem.*, 2013, **52**, 2637-2647.

40. P. F. Li, C. L. Hu, F. Kong and J. G. Mao, *Angew.Chem. Int. Ed.*, 2023, **62**, e202301420.

41. E. P. Lee, S. Y. Song, D. W. Lee and K. M. Ok, *Inorg. Chem.*, 2013, **52**, 4097-4103.

42. M. Shang and P. S. Halasyamani, *J. Solid State Chem.*, 2020, **282**, 121121.

43. R. Robert, V. Balisetty, K. Mohanrao, M. Mannamala, S. Mangalassery, D. N. Rao and K. Vidyasagar, *Inorg. Chem.*, 2023, **62**, 7890-7897.